Red tide mortality on gag grouper from 2002-2018 generated by an Ecospace model of the West Florida Shelf

Daniel Vilas, David Chagaris, and Joe Buczkowski

SEDAR72-WP-01

4 September 2020
Updated: 17 December 2020
Updated: 29 January 2021

Please cite this document as:

Vilas, Daniel, David Chagaris, and Joe Buczkowski. 2020. Red tide mortality on gag grouper from 2002-2018 generated by an Ecospace model of the West Florida Shelf. SEDAR72-WP-01. SEDAR, North Charleston, SC. 17 pp.

Red tide mortality on gag grouper from 2002-2018 generated by an Ecospace model of the West Florida Shelf

A working paper for the SEDAR 72 stock assessment of gag grouper in the Gulf of Mexico

Daniel Vilas[1], David Chagaris[1], and Joe Buszowski[2]

[1]University of Florida; [2]Ecopath International Initiative

Introduction

It is widely recognized the importance of considering abiotic factors, human-induced or natural, when exploring marine population dynamics, geographic ranges, or ecosystem effects (Pinsky et al. 2020). On the West Florida Shelf, red tide events are considered a major concern because of their complex dynamics, impacts at multiple trophic levels, and increasing frequency (Walsh and Steidinger 2001). Red tide events are harmful algal blooms (HABs) that produce toxicity on the coastal waters and are promoted by several factors including anthropogenic and natural such as nutrient runoff and upwelling. These episodic events negatively affect the economy, human health, and ecology, and future scenarios predicted an increase in the frequency and maybe the severity of red tide events (Bechard 2019; Griffith and Gobler 2020).

Because of the impacts and natural complexity of red tide events, the scientific community has been striving to estimate and predict impacts on marine ecosystems. For instance, ecosystem modeling studies (Gray DiLeone and Ainsworth 2019; Perryman et al. 2020) included red tide events as a pseudo fishing fleet and suggested that mortality due to red tide events may cause changes in the community structure and cascading effects on the food web. However, some fishery management plans face challenges that require a spatial ecosystem focus to achieve ecosystem-based fishery management (EBFM) (Chagaris et al. 2019).

Several environmental factors such as temperature have been incorporated into the decision-making process through stock assessments. Other factors causing episodic natural mortality events have been incorporated in such processes, for example, cold-kill and red tide events. In the Gulf of Mexico, red grouper and (*Epinephelus morio*) and gag grouper (*Mycteroperca microlepis*) stock assessments recognized red tide mortality (SEDAR 2014, 2019). The current fisheries management framework calls for a more comprehensive consideration of episodic natural mortality events, habitat effects, and spatial holistic approach (Chagaris et al. 2019). Because of the inclusion of those considerations, ecosystem models can serve as potential tools to evaluate the impact of environmental stressors such as HABs in terms of mortality rates and biomass loss to afterward incorporate into stock assessment models.

The mortality rate associated with red tides can be substantial on certain fish species. For gag grouper, red tide mortality (M_{RT}) in 2005 was estimated between about 0.35 and 0.99 in the previous three stock assessments (SEDAR 2009, 2014, and 2016), which is 2 to 5 times higher than baseline natural mortality rates. Thus, recent stock assessments have estimated severe, although highly variable, effects of red tide on gag populations. Similarly, red tide was included in the last stock assessment of red grouper and was estimated to kill approximately 43.8% of the total biomass in 2005 (SEDAR 2015). In the last two stock assessments for gag and red grouper (SEDAR 2016, 2018), red tide was treated as a pseudo, discard only, fishing fleet. Selectivity was assumed to be constant across size and age. During years in which severe red tide events occurred, a red tide mortality rate was estimated to improve the fit to indices of abundance. In

this approach, a decision must be made about which years to 'turn on' for red tide effects. For gag, this included 2005 and for red grouper this included 2005 and 2014. Subsequent assessments will also likely include 2018 as an event year. An alternative approach would be to input a continuous time series of relative red tide mortality, ideally for each age, in order to estimate mortality in all years, but constrained by the input time series. In this working paper, we provide age-specific time series of red tide mortality rates for gag grouper from 2002-2018 using an Ecospace model of the West Florida Shelf (WFS).

Methods

The WFS Ecospace model

Ecospace is the the spatially explicit simulation module of the Ecopath with Ecosim (EwE) software package. The WFS Ecospace model includes 17 fishing fleets and 83 functional groups (FGs) which represent individual species, life stages, or groups of functionally similar species. The WFS Ecospace model encompasses an area ranging from 30.5 to 25 degrees latitude and from -87.5 to -81 degrees longitude. It is simulated over a map with a spatial resolution of 10 minutes, (~20km) containing 38 rows x 40 columns from 1985 to 2018 at monthly steps.

Ecospace incorporates a habitat capacity model that represents the quality of each cell for each functional group based on the FGs' response to environmental drivers (Christensen et al., 2014). In Ecospace, a biomass fraction moves to adjacent cells depending on the habitat quality computed with the habitat capacity model. Depth, rugosity, sea surface temperature (SSS), sea bottom temperature (SBT), sea surface salinity (SSS), and red tide were incorporated in the WFS Ecospace model using the Ecospace spatiotemporal framework (Steenbeek et al., 2013). To obtain environmental response functions, full generalized additive models (GAMs) were fitted to fisheries-independent data from multiple surveys including all available environmental variables. Negative binomial and binomial families were investigated using either biomass or presence/absence and binomial was selected because it produced more informative environmental response functions. Only the significant environmental variables were included as response functions for each FG in the WFS Ecospace model. For example, SBT response functions were assigned to demersal and reef-associated FGs while SST response functions were assigned to pelagic FGs. When a FG was caught by multiple surveys, the response function from the survey with the highest frequency of occurrence was used. SEAMAP trawling survey data were used for demersal and benthic FGs. The FWC and NOAA reef fish camera survey data were used for reef-associated FGs. The FWC baitfish cruise survey was used for medium and small pelagic FGs. NMFS bottom longline survey data were used for some adult reef fish and elasmobranchs FGs. Baseline dispersal rates (km/y) were estimated from movement rates in published tagging studies. When dispersal rates were not available, dispersal rates were set based on the general "300-30-3" rule which assumes 300 km/y for pelagic and medium and large reef-associated FGs, 30 km/y for small reef-associated and demersal FGs, and 3 km/y for benthic and planktonic FGs.

Ecospace model stability was achieved in a stepwise approach by ensuring persistence and a non-exponential increase of FGs over time. Stability was checked for each model configuration in terms of the incorporation of environmental variables, going from a static Ecospace model that incorporates depth and rugosity to the fully spatial dynamic Ecospace model that includes static and monthly environmental variables (SST, SSB, SSS, primary production and red tide). To validate Ecospace simulation, long-term Ecospace biomass maps were compared with predicted probability of occurrence maps from GAMs for the most relevant FGs. Long-term Ecospace

biomass maps were obtained by averaging maps of all monthly steps. Schoener's D and I similarity index, and Spearman correlation were used for comparing each pair of maps for each FG.

Creation of Red tide maps

K. brevis cell concentration (cells/L) data collected by Florida Fish and Wildlife Research Institute Harmful Algal Bloom monitoring group (FWRI-HAB) were interpolated over the entire WFS using ordinary kriging. For each month and sample location we obtained the maximum observed *K. brevis* cell concentration and performed ordinary kriging for months when there were at least 5 sites with maximum concentrations greater than or equal to 1,000 cells/L. The 'automap' [R] package (Hiemstra et al. 2009) was used to fit the variogram model to the log-transformed monthly observed maximum cell concentrations at each sample location. Several variogram model types were tested, including the commonly used spherical, exponential, and matern (M. Stein's parameterization) models, and the model with the smallest residual sum of squares in the sample variogram was selected. The selected model and data were used to predict cell concentrations over a spatial grid and then back-transformed. Monthly normalized fluorescent line height (nFLH) grids derived from the MODIS-Aqua satellite (NASA Goddard Space Flight Center 2020) were used to define the spatial extent and duration of harmful algal blooms. Monthly maps of the WFS with HAB polygons were generated from nFLH based on a threshold detection value 0.02 mW cm^{-2} um^{-1} sr^{-1} (Hu et al., 2005) Lastly, the kriged maps were clipped to the HAB polygons and resampled to match the resolution of the Ecospace model. The monthly red tide concentration maps were then loaded into the Ecospace spatial-temporal framework as a time series of spatial ASCII files.

Simulating red tides effects in Ecospace

Red tide response functions were defined to generate direct mortality and sub-lethal effects (i.e. reduced feeding & growth, and movement) of red tides. The red tide mortality response determined the proportion of biomass killed (*P*) in each grid cell and monthly time step, *t*, as a function of *K. brevis* cell concentration, *x*. The mortality response functions assumed a logistic curve with a slope, *b*, that were computed from multiple scalar values (1,000, 20,000, 50,000 and 100,000) and multiple inflection points, *c*, of 50,000, 100,000, 200,000, 300,000 and 400,000 cells/L, representing multiple sensitivity levels and 20 red tide mortality response functions (Figure 1, Table 2).

$$P_t = \frac{1}{1 + \left(\frac{x_t}{c}\right)^{-b}}$$

The proportion killed was converted to an annual instantaneous mortality rate, $\widehat{P_t}$, and scaled to the Ecopath other mortality rate, $M0_{base}$, to return the other mortality multiplier term, *M0mult*, for a grid cell and monthly time step.

$$\widehat{P_t} = -\ln(1 - P_t) * 12$$

$$M0mult_t = \frac{\widehat{P_t}}{M0_{base}}$$

The foraging responses were used to simulate sub-lethal effects and serve two roles in the simulations. First, they reduce the foraging arena size in affected grid cells, which thereby reduces consumption and biomass growth. Additionally, the reduced foraging capacity in an affected cell will increase the movement rate out of that cell. This allows fish to move away from red tide blooms and may mitigate direct mortality losses if cells with suitable habitat are nearby. The red tide foraging response was defined using a logistic curve that decreased with red tide cell concentrations (Figure 2). The foraging responses had lower inflections points (from 12,500 to 300,000 cells/L) than the mortality responses since sub-lethal effects and avoidance response are likely to be experienced at lower *K. brevis* concentrations (i.e. fish will move or stop feeding before they die). Three foraging curves were generated for each value of *c*, at multiple sensitivity levels of 25%, 50%, and 75% of the mortality inflection point. The slope for each foraging response curve was scaled relative to the inflection point, using a multiplier of $-5e^{-5}$, such that the shape of the curve did not change, while its position on the x-axis did (Figure 2, Table 2). This resulted in 15 foraging response functions (three foraging response curves for each mortality inflection point function) that represent multiple sensitivity levels (Figure 2).

For each species or FG the total biomass loss from all mortality sources in each grid cell and month was calculated as

$$loss_t = predation_t + \left(M0_{base} \cdot M0mult_t \cdot \left(1 - M0_{pred} + M0_{pred} \cdot FT_t\right) + E_t + F_t\right) \cdot B_t$$

Where $M0_{pred}$ is a fixed constant representing the fraction of other mortality sensitive to changes in foraging time (*FT*), *E* is an emigration rate, *F* is fishing mortality, and *B* is biomass. In these scenarios, $M0_{pred}$ and *E* are zero for all groups. Predation losses are determined through foraging arena equations and fishing mortality in a grid cell is determined from the effort occurring in that cell, which is distributed spatially using a gravity model. The biomass loss due to red tides for each FG, grid cell, and monthly time step is calculated as

$$RTloss_t = B_t \cdot \frac{\widehat{P}_t}{12}$$

A monthly time series of red tide mortality was calculated by dividing the total red tide loss over all map cells, m, by the total biomass.

$$MRT_t = \frac{\sum_m RTloss_t}{\sum_m B_t}$$

An annual index of red tide mortality was calculated as the average MRT over months

$$MRT_y = \frac{\sum_y MRT_t}{12}$$

Red tide scenarios

We ran a total of 160 Ecospace scenarios representing different sensitivities and combinations of response functions. The first 20 only included the mortality response functions (five sensitivities with four slopes each), while the next 60 included three foraging responses for

each of the 20 mortality responses representing the different sensitivities to sub-lethal effects, relative to each mortality curve. The 80 configurations were run once with red tide response functions applied only to gag grouper age stanzas, and then again with response functions applied to all consumer groups (Table 1). We used the Ecospace Console Application that is a command-line version of EwE that runs Ecospace in a command-line interpreter (such as R) without a user interface which allowed us to standardize the process and decrease simulation time by automatizing the simulations and so avoiding errors related to manual editing steps.

Evaluation

The goodness of each fit was evaluated by two criteria. First, comparing 2005 red tide loss rates predicted from Ecospace with the estimated loss rate in 2005 from the last SEDAR assessment (SEDAR 2016). In that SEDAR assessment, the proportion of gag age 1+ killed was 0.77, with an estimated standard deviation of 0.06. We assumed that predicted values within 2 standard deviations of the mean, 0.65-0.99, were considered acceptable runs. Second, predicted biomass was compared with the CPUE indices from SEDAR 33 update assessment. To do that, selectivity information from this SEDAR assessment was used to convert biomass-at-age from Ecospace to vulnerable biomass series specific for each index. Root mean squared error (RMSE) was computed for each run in this comparison, including run0 or baseline run in which red tide effects were not applied. Acceptable RMSE values were considered within 10% of the lowest RMSE. Valid runs were identified by meeting both criteria and screened from the larger set of runs for calculating the mean index and confidence intervals.

Ecospace Spatial Validation

For validation purposes, we selected the WFS Ecospace model with the best fit applying red tide response functions to all consumer groups. The validation process of the WFS Ecospace model in which we investigated how well model spatial predictions match observations was carried out at two different levels. First, long-term Ecospace biomass maps were compared with the predicted probability of occurrence maps from generalized additive models (GAMs) for the most relevant FGs. GAMs were fitted by using empirical data from multiple surveys (the SEAMAP trawling, the FWC and NOAA reef fish camera, the FWC baitfish cruise, the NMFS bottom longline, and the ROV abundance estimates from the Great Red Snapper Count). Long-term Ecospace biomass maps were obtained by averaging maps of all monthly steps. Jaccard coefficient, Schoener's D and I similarity indices, and Spearman correlation index will be used for comparing each pair of maps for each FG.

Similarly, red tide effects were spatially validated by comparing the percent of change in terms of marine organisms' abundance. First, red tide events were spatiotemporally matched with empirical observations from survey data to capture observed red tide mortality effects. Selected survey data were the SEAMAP trawling survey for June (no red tide) and October 2015 (red tide) and the NMFS bottom longline survey for August 2014 (red tide). For the trawling survey, the observed red tide effect was calculated by comparing the average abundance of marine organisms in the Charlotte Harbour area between both months. For the bottom longline, the observed red tide effect was calculated by comparing the average abundance of marine organisms inside and outside the red tide affected area. Afterward, both red tide effects were compared with the predicted effects by the WFS Ecospace model.

Results & Discussion

Based on both selection criteria, 133 out of 160 runs were selected and included in the mean index calculation. The mean red tide mortality rate fluctuated over time with the highest values in 2005 followed by 2006, 2018, 2012, and 2015-2016 (Table 3, Figure 3). Mortality rates were generally higher for younger age stanzas, except for 2005 when the bloom persisted far offshore. In years where the bloom remained close to shore (2006, 2012, 2016, and 2018) age-0 gag was more strongly impacted. Gag 5+ was predicted to have the lowest mean red tide mortality rate over time and the model only estimated a noticeable red tide mortality rate peak in 2005 with an $M_{RT} = 0.151$. Additionally, the model estimated higher uncertainty around the mortality rate in years when moderate to severe red tides occurred (Figure 3).

When comparing the 2005 mortality rate from Ecospace runs with the SEDAR 33 estimated mortality in 2005, several runs fall within the +/- 2sd threshold. In general, the runs assuming medium sensitivities with both mortality and foraging responses applied produced 2005 estimates within this range (Figure 4). Runs with RMSE that were no more than 10% higher than the minimum RMSE were also obtained in the medium sensitivity scenarios (Figure 5), with fewer acceptable runs when red tide responses were applied to all functional groups compared to when responses were only applied to gag. Among all runs, we selected run 134 to demonstrate validation because it obtained the best fit in the evaluation process and applied mortality and foraging red tide response functions to all consumer groups. Vulnerable biomass predictions of Ecospace selected run were similar to the ones estimated in SEDAR 33 update assessment (SEDAR 2016) assessment (Figure 6). These results also highlighted the ability of Ecospace to capture the biomass decline in 2005 due to a severe red tide event, and the subsequent increase in recruitment displayed on gag 0.

The similarities between Ecospace biomass and that predicted in SEDAR 33U is striking (Figure 6). Interannual variability of biomass in the stock assessment is mostly driven by fishing mortality rates and recruitment deviations, whereas in Ecospace the dynamics are driven by fishing effort, red tide, and trophic interactions. The ability for Ecospace to replicate those patterns suggests that red tides are playing a dominant role in structuring this population. In the stock assessment model, interannual variability in the data (index trends and length/age compositions) is interpreted as changes in fishing mortality and recruitment deviations, but this analysis indicates that inter-annual variation could be attributed to fishing and red tides instead. Ecospace predictions suggested that red tides may be driving recruitment variability for gag. High recruitment of juveniles is believed to follow red tide events and Ecospace was able to predict these increases only in runs where red tide is applied to all functional groups (Figure 6). This suggest that increases in recruitment following red tides is a result of trophic dynamic processes such as reduced competition for food and lower predation rates of juvenile gag.

In the validation analysis, predictions from Ecospace showed a negative percent of change due to red tide effects in the selected time as pointed out by empirical data (Figure 7). However, these measures differed on the magnitude of the abundance percent of change, especially for the SEAMAP trawling measures in 2015. These validations are considered preliminary, and more work is needed to compare red tide effects from the WFS Ecospace model with empirical data by species or functional group basis.

Tables

Table 1. Set of 160 red tide scenarios evaluated with the WFS Ecospace model under different assumptions about sensitivity and effects on other functional groups.

Sensitivity (i.e. response fxns)	**response applied to gag stanzas only**		**response applied to all consumer groups**	
	M0	**M0+foraging**	**M0**	**M0+foraging**
high	run1-run4	run21-run32	run81-run84	run101-run112
medium-high	run5-run8	run33-run44	run85-run88	run113-run124
medium	run9-run12	run45-run56	run89-run92	run125-run136
medium-low	run13-run16	run57-run68	run93-run96	run137-run148
low	run17-run20	run69-run80	run97-run100	run149-run160

Table 2. Logistic response curve inflection points (c) and slopes (b) for the red tide mortality and foraging response functions.

	low		**medium low**		**medium**		**medium high**		**high**	
mortality response shape	**c**	**b**	**c**	**b**	**c**	**b**	**c**	**b**	**c**	**b**
flat	400,000	400	300,000	300	200,000	200	100,000	100	50,000	50
mediumflat	400,000	20	300,000	15	200,000	10	100,000	5	50,000	2.5
mediumsteep	400,000	8	300,000	6	200,000	4	100,000	2	50,000	1
steep	400,000	4	300,000	3	200,000	2	100,000	1	50,000	0.5
Foraging Response Parameters										
low sensitivity	300,000	-15	225,000	-11.25	150,000	-7.5	75,000	-3.75	37,500	-1.875
medium sensitivity	200,000	-10	150,000	-7.5	100,000	-5	50,000	-2.5	25,000	-1.25
high sensitivity	100,000	-5	75,000	-3.75	50,000	-2.5	25,000	-1.25	12,500	-0.625

Table 3. Estimated mean and 95% confidence interval (CI) red tide mortality rate of 133 selected runs for each gag stanza.

	gag 0		gag 1		gag 2		gag 3		gag 4		gag 5+	
Years	**mean**	**95% CI**	**mean**	**95% CI**	**mean**	**95% CI**	**mean**	**95% CI**	**mean**	**95% CI**	**mean**	**95% CI**
2002	0.045	0.001 - 0.099	0.038	0.001 - 0.078	0.035	0.001 - 0.07	0.033	0.001 - 0.066	0.021	0.002 - 0.043	0.002	0.000 - 0.006
2003	0.077	0.013 - 0.180	0.072	0.010 - 0.143	0.071	0.009 - 0.145	0.082	0.010 - 0.170	0.078	0.005 - 0.163	0.015	0.001 - 0.030
2004	0.021	0.000 - 0.044	0.018	0.000 - 0.039	0.015	0.000 - 0.032	0.014	0.000 - 0.032	0.005	0.000 - 0.011	0.000	0.000 - 0.001
2005	0.762	0.235 - 1.214	0.743	0.236 - 1.144	0.650	0.222 - 1.078	0.709	0.247 - 1.145	0.669	0.220 - 1.105	0.151	0.045 - 0.256
2006	0.686	0.242 - 1.221	0.390	0.148 - 0.651	0.249	0.105 - 0.399	0.361	0.135 - 0.605	0.108	0.039 - 0.175	0.002	0.001 - 0.004
2007	0.035	0.005 - 0.086	0.039	0.008 - 0.078	0.039	0.009 - 0.064	0.055	0.011 - 0.081	0.046	0.011 - 0.083	0.001	0.000 - 0.002
2008	0.002	0.000 - 0.006	0.002	0.000 - 0.006	0.001	0.000 - 0.004	0.001	0.000 - 0.002	0.000	0.000 - 0.001	0.000	0.000 - 0.000
2009	0.029	0.004 - 0.061	0.033	0.005 - 0.061	0.033	0.006 - 0.064	0.032	0.008 - 0.053	0.032	0.005 - 0.056	0.002	0.001 - 0.004
2010	0.000	0.000 - 0.001	0.000	0.000 - 0.001	0.000	0.000 - 0.001	0.000	0.000 - 0.000	0.000	0.000 - 0.000	0.000	0.000 - 0.000
2011	0.110	0.023 - 0.206	0.104	0.027 - 0.194	0.098	0.027 - 0.188	0.094	0.029 - 0.173	0.073	0.025 - 0.127	0.007	0.002 - 0.011
2012	0.257	0.074 - 0.468	0.154	0.047 - 0.297	0.088	0.031 - 0.139	0.104	0.037 - 0.159	0.072	0.026 - 0.130	0.008	0.003 - 0.014
2013	0.034	0.004 - 0.083	0.015	0.002 - 0.036	0.009	0.001 - 0.019	0.010	0.002 - 0.018	0.005	0.001 - 0.009	0.001	0.000 - 0.002
2014	0.038	0.004 - 0.067	0.052	0.006 - 0.087	0.048	0.007 - 0.080	0.056	0.011 - 0.108	0.051	0.011 - 0.093	0.011	0.004 - 0.020
2015	0.115	0.026 - 0.197	0.099	0.025 - 0.157	0.099	0.026 - 0.171	0.114	0.032 - 0.234	0.124	0.036 - 0.212	0.009	0.003 - 0.016
2016	0.215	0.029 - 0.414	0.145	0.020 - 0.263	0.107	0.013 - 0.209	0.110	0.015 - 0.209	0.075	0.012 - 0.201	0.005	0.001 - 0.013
2017	0.027	0.003 - 0.058	0.018	0.003 - 0.044	0.011	0.003 - 0.025	0.010	0.001 - 0.025	0.009	0.004 - 0.014	0.000	0.000 - 0.001
2018	0.316	0.102 - 0.604	0.247	0.078 - 0.459	0.170	0.061 - 0.328	0.180	0.067 - 0.321	0.195	0.073 - 0.318	0.032	0.011 - 0.048

Figures

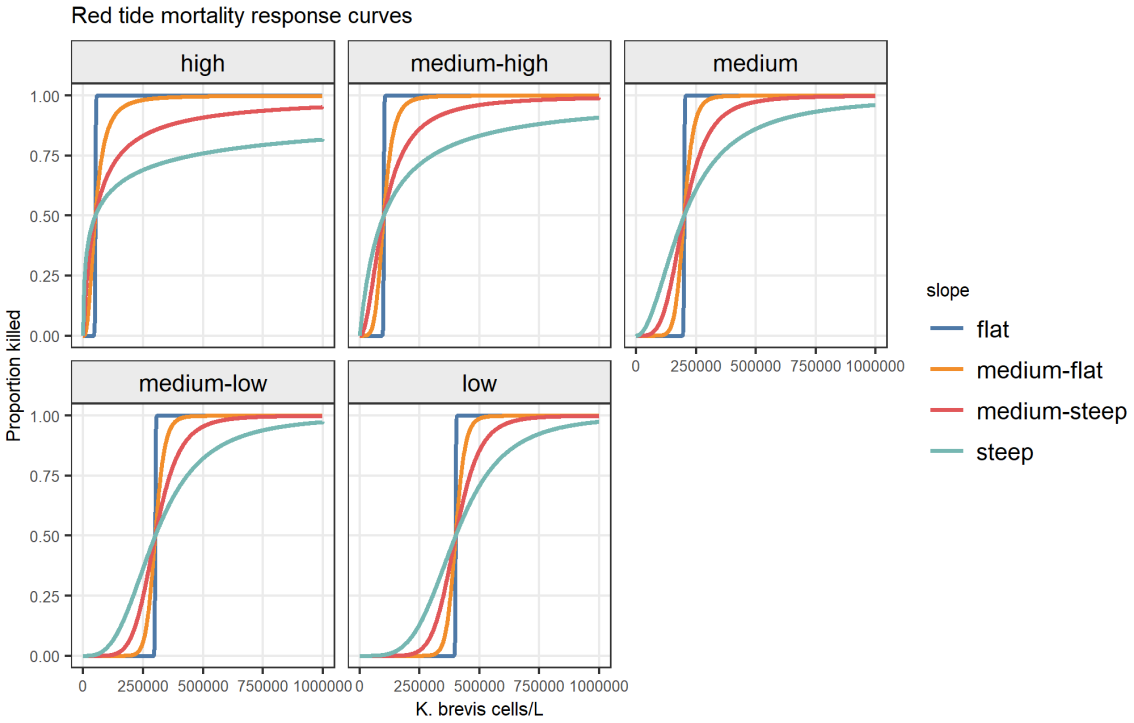

Figure 1. Red tide mortality response curves used in the WFS Ecospace model, representing multiple sensitivities to red tide.

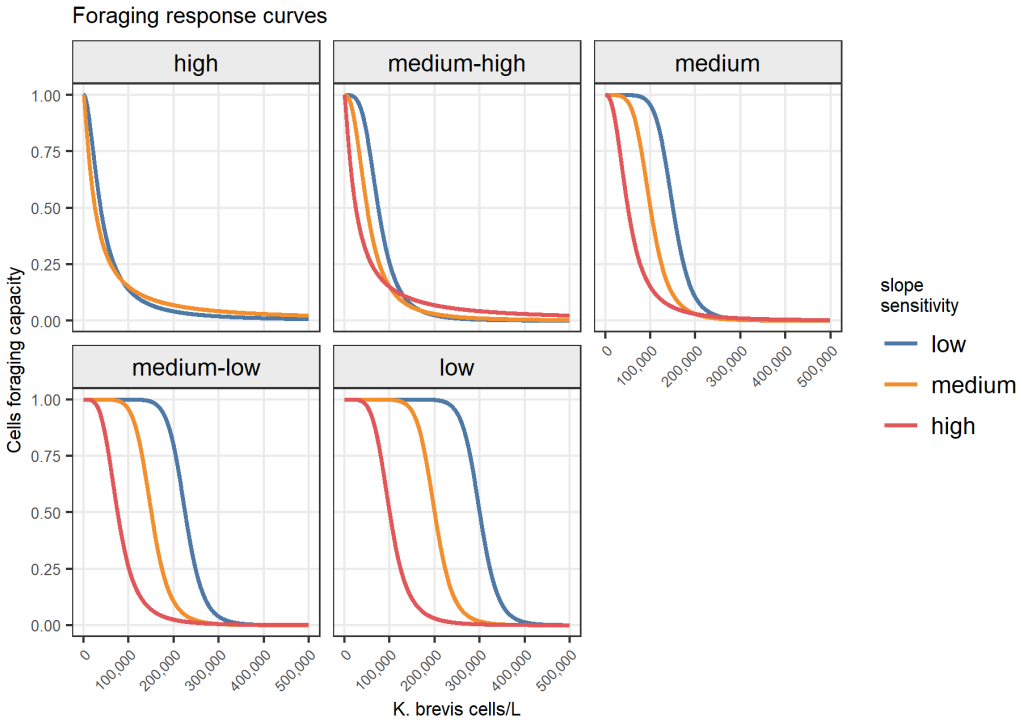

Figure 2. Foraging response curves used in the WFS Ecospace model, representing multiple sensitivities to red tide.

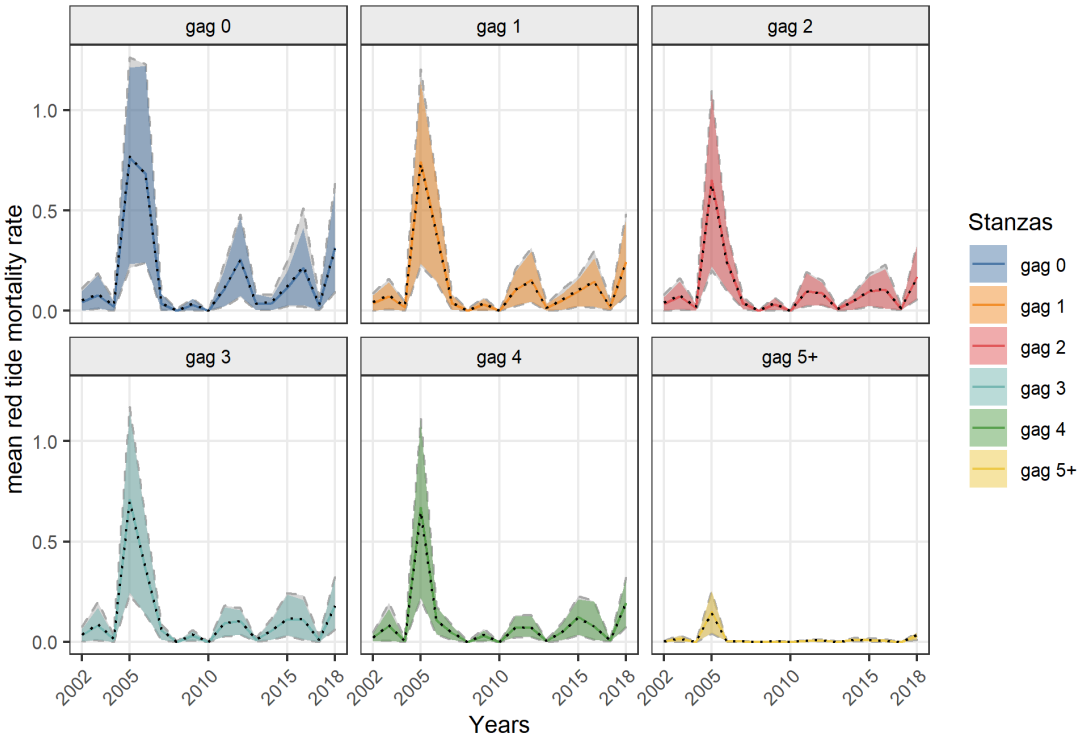

Figure 3. Time series of estimated mean and 95% confidence interval red tide mortality for gag grouper from 2002-2018 generated by the WFS Ecospace model. Colored lines and shades represent estimates for selected runs. Black dotted line and grey shades represent estimates for all runs.

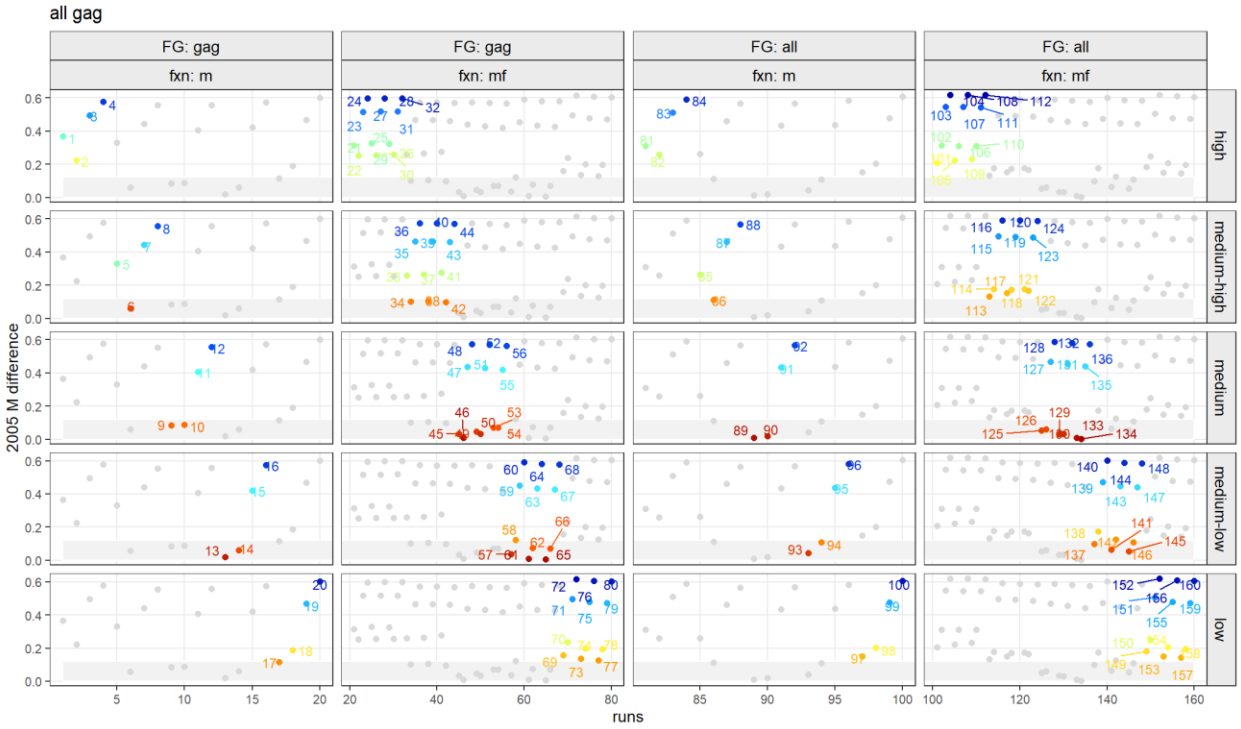

Figure 4. Absolute difference on gag grouper mortality in 2005 estimated in SEDAR 33 and each of the 160 runs classified by sensitivity, functional group applied (FG), and response functions applied (m: mortality; mf: mortality and foraging). Color intensities represent the magnitude of the estimate (red: high; blue: low). Numbers represent run numbers (for detailed information on runs see Table 1).

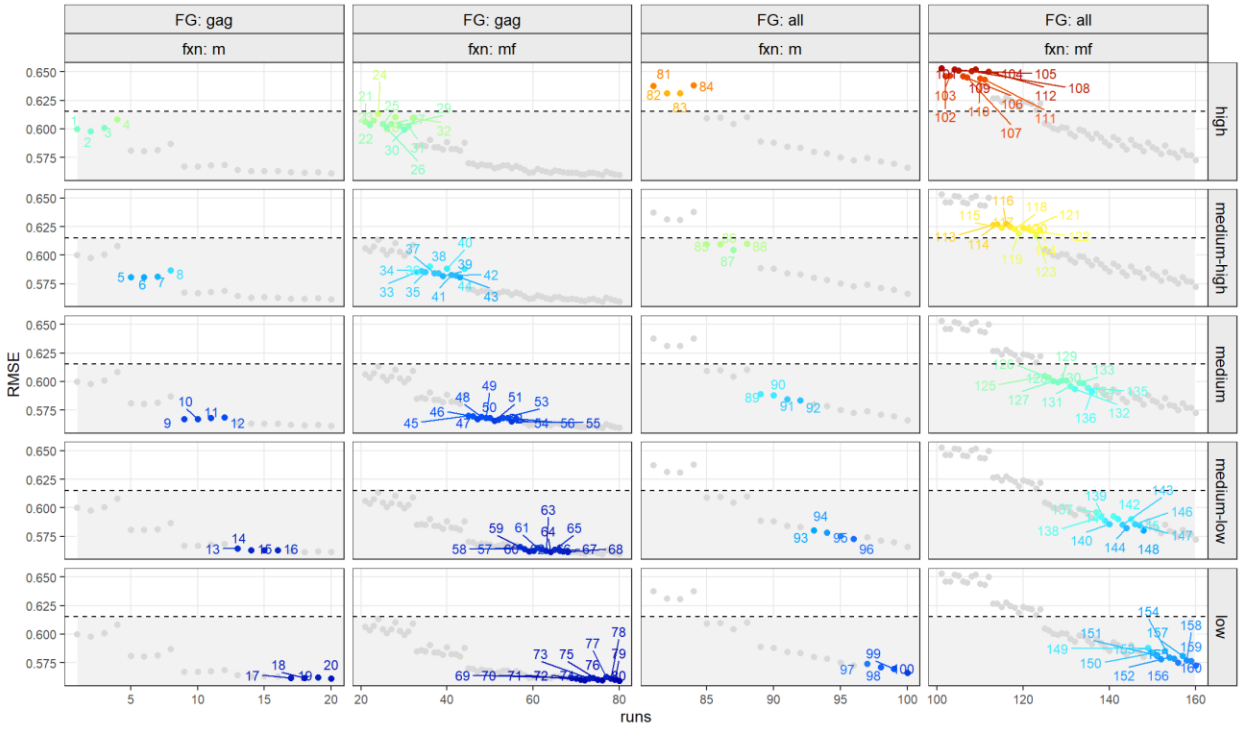

Figure 5. Root mean squared error (RMSE) for 160 runs by sensitivity, functional group (FG) in which response functions were applied and applied functions (m: mortality; mf: mortality and foraging). Color intensities represent RMSE value (red: high; blue: low). Numbers represent run numbers. Dashed lines represent the threshold based on run0 RMSE. Grey rectangles represent acceptable values for RMSE (for detailed information on runs see table 1).

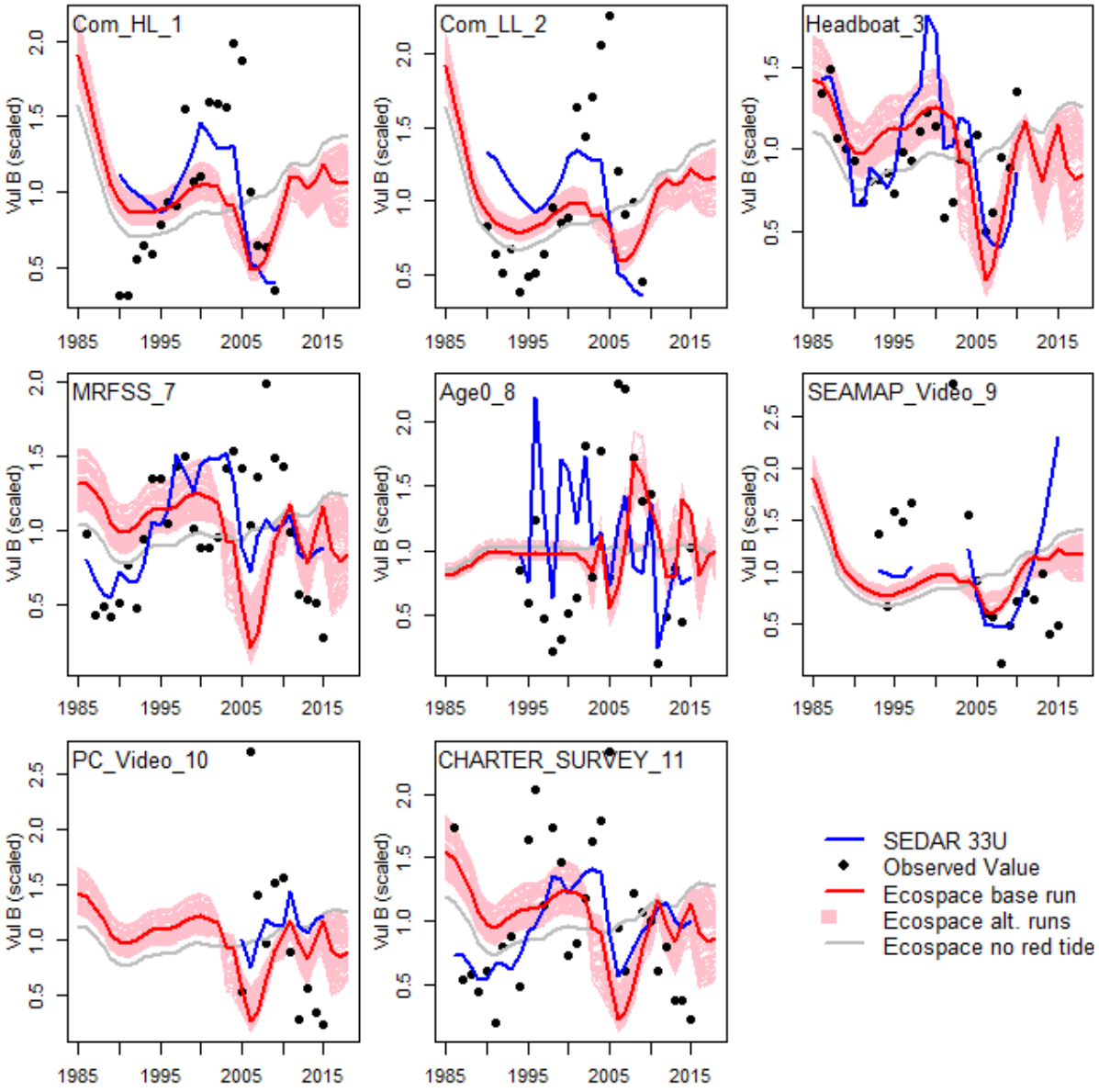

Figure 6. Vulnerable biomass prediction from Ecospace run 134 (red) and estimated vulnerable biomass from SEDAR 33 update assessment overlaid on the observed index of abundance values (points) and all runs from WFS Ecospace (pink). The gray line represents the Ecospace scenario with no red tide effects included.

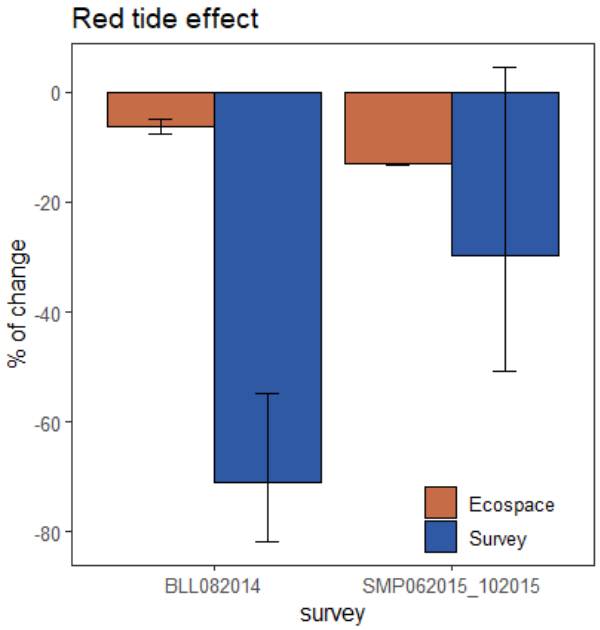

Figure 7. Percent of abundance change due to red tide effects in bottom longline (BLL) and SEAMAP trawling (SMP) survey for Ecospace (blue) and Survey (red) data. Error bars represent standard error.

References

Bechard, A. 2019. Red tide at morning, tourists take warning? County-level economic effects of HABS on tourism dependent sectors. Harmful Algae 85:101689.

Chagaris, D., S. Sagarese, N. Farmer, B. Mahmoudi, K. de Mutsert, S. VanderKooy, W. F. Patterson, M. Kilgour, A. Schueller, R. Ahrens, and M. Lauretta. 2019. Management challenges are opportunities for fisheries ecosystem models in the Gulf of Mexico. Marine Policy 101:1–7. Pergamon.

Christensen, V., Coll, M., Steenbeek, J., Buszowski, J., Chagaris, D., and Walters, C. (2014). Representing Variable Habitat Quality in a Spatial Food Web Model. *Ecosystems* 17**,** 1397-1412.

Gray DiLeone, A. M., and C. H. Ainsworth. 2019. Effects of Karenia brevis harmful algal blooms on fish community structure on the West Florida Shelf. Ecological Modelling 392:250–267.

Griffith, A. W., and C. J. Gobler. 2020. Harmful algal blooms: a climate change co-stressor in marine and freshwater ecosystems. Harmful Algae 91:101590. Elsevier.

Hiemstra, P. H., E. J. Pebesma, C. J. W. Twenhöfel, and G. B. M. Heuvelink. 2009. Real-time automatic interpolation of ambient gamma dose rates from the Dutch radioactivity monitoring network. Computers & Geosciences 35(8):1711–1721. Elsevier.

Hu, C., Muller-Karger, F.E., Taylor, C.J., Carder, K.L., Kelble, C., Johns, E., and Heil, C.A. (2005). Red tide detection and tracing using MODIS fluorescence data: A regional example in SW Florida coastal waters. *Remote Sensing of Environment* 97**,** 311-321.

NASA Goddard Space Flight Center. 2020. MODIS-Terra Ocean Color Data; NASA Goddard Space Flight Center, Ocean Ecology Laboratory, Ocean Biology Processing Group. https://oceanwatch.pifsc.noaa.gov/erddap/.

Perryman, H. A., J. H. Tarnecki, A. Grüss, E. A. Babcock, S. R. Sagarese, C. H. Ainsworth, and A. M. G. DiLeone. 2020. A revised diet matrix to improve the parameterization of a West Florida Shelf Ecopath model for understanding harmful algal bloom impacts. Ecological Modelling 416:108890. Elsevier.

Pinsky, M. L., R. L. Selden, and Z. J. Kitchel. 2020. Climate-Driven Shifts in Marine Species Ranges: Scaling from Organisms to Communities. Annual Review of Marine Science 12(1):153–179. Annual Reviews.

SEDAR. 2009. SEDAR 10 Update – Gulf of Mexico gag grouper stock assessment report. SEDAR, North Charleston, SC. Available online: www.sedarweb.org.

SEDAR. 2014. SEDAR 33 – Gulf of Mexico gag grouper stock assessment report. SEDAR, North Charleston, SC. Available online: www.sedarweb.org.

SEDAR. 2016. SEDAR 33 Update – Gulf of Mexico gag grouper stock assessment report. SEDAR, North Charleston, SC. Available online: www.sedarweb.org.

SEDAR. 2018. SEDAR 61 – Gulf of Mexico red grouper stock assessment report. SEDAR, North Charleston, SC. Available online: www.sedarweb.org.

SEDAR. 2019. SEDAR 61 - Gulf of Mexico red grouper stock assessment report. North Charleston, South Carolina.

Steenbeek, J., Coll, M., Gurney, L., Mã©Lin, F.D.R., Hoepffner, N., Buszowski, J., and Christensen, V. (2013). Bridging the gap between ecosystem modeling tools and geographic information systems: Driving a food web model with external spatial-temporal data. *Ecological Modelling* 263**,** 139-151.

Walsh, J. J., and K. A. Steidinger. 2001. Saharan dust and Florida red tides: the cyanophyte connection. Journal of geophysical research: Oceans 106(C6):11597–11612. Wiley Online Library.